Separation Science and Technology

Publication details, including instructions for authors and subscription information:
http://www.informaworld.com/smpp/title~content=t713708471

Soil Clean Up by in-situ Aeration. III Passive Vent Wells, Recontamination, and Removal of Underlying Nonaqueous Phase Liquid

David J. Wilson[a]; Ann N. Clarke[b]; Robert D. Mutch Jr.[b]
[a] DEPARTMENT OF CHEMISTRY VANDERBILT, UNIVERSITY NASHVILLE, TENNESSEE [b] ECKENFELDER, INC., NASHVILLE, TENNESSEE

To cite this Article Wilson, David J. , Clarke, Ann N. and Mutch Jr., Robert D.(1989) 'Soil Clean Up by in-situ Aeration. III Passive Vent Wells, Recontamination, and Removal of Underlying Nonaqueous Phase Liquid', Separation Science and Technology, 24: 12, 939 — 979

To link to this Article: DOI: 10.1080/01496398908049883

URL: http://dx.doi.org/10.1080/01496398908049883

SEPARATION SCIENCE AND TECHNOLOGY, 24(12 & 13), pp. 939-979, 1989

Soil Clean Up by *in-situ* Aeration. III Passive Vent Wells, Recontamination, and Removal of Underlying Nonaqueous Phase Liquid

DAVID J. WILSON

DEPARTMENT OF CHEMISTRY
VANDERBILT UNIVERSITY
NASHVILLE, TENNESSEE 37235

ANN N. CLARKE and ROBERT D. MUTCH JR.

ECKENFELDER, INC.
NASHVILLE, TENNESSEE 37228

Abstract

A mathematical model for simulating the operation of soil vapor stripping wells for the removal of volatile contaminants is extended to examine the possible benefits of using passive vent wells to increase clean-up rates. Contrary to expectation, these do not generally seem to improve soil vapor stripping performance. The model is also used to examine recontamination of a vapor stripped vadose zone by vaporization and diffusion of underlying nonaqueous phase liquid and to investigate the possibility of removal of underlying light nonaqueous phase liquid pools by vapor stripping from the vadose zone.

INTRODUCTION

The advantages to be obtained from the use of soil vapor stripping, where it is applicable, have been described in our earlier papers (*1*, *2*). Recently the technique has become relatively commonly used, and has been the subject of several laboratory and field-scale studies. Laboratory studies include Wootan and Voynick's experiments on the vapor stripping of gasoline from a large-scale sand aquifer (*3*), and Clarke's report on the vapor stripping of several volatile organics in laboratory columns (*4*). Woodward-Clyde Consultants (*5*) described a pilot scale vapor stripping study near Tacoma, Washington. Anastos et al. (*6*) reported on a pilot study of soil vapor stripping for the removal of trichloroethylene and other volatiles at the Twin Cities Army Ammunition Plant, Minnesota. Crow, Anderson, and Minugh (*7*) presented results on soil vapor stripping at a petroleum fuels terminal. Bailey and Gervin (*8*) reported on a pilot study of *in-situ* soil vapor stripping of chlorinated solvents, and Lord (*9*) presented data on the vapor stripping of gasoline from soil in the vicinity of streets and buildings. Recently Terra Vac (*10*) carried out a demonstration test at Groveland, Massachusetts.

We have described mathematical models for simulating the operation of lab columns and field-scale vapor stripping wells, and have discussed the use of the lab column data to obtain parameters for the field-scale model (*1*, *2*, *11*, *12*). The effects of impermeable obstacles, impermeable overlying caps, well depth, well packing radius, and evaporative cooling of the soil were discussed.

In the present paper we examine the effects of passive wells on the performance of the soil vapor stripping technique, the extent and rate of recontamination from material below the vadose zone, and the possibility of vapor stripping pools of light nonaqueous phase liquid (LNAPL) lying at the bottom boundary of the vadose zone. The model used here has been discussed in detail in our earlier papers, to which the reader is referred for derivations, etc. We use the same notation here as in our previous work wherever possible.

ANALYSIS

Our model is divided into two principal sections; the calculation of the gas velocity field in the soil being stripped and the calculation of the movement of the volatile contaminants under the influence of this velocity field. The gas pressures present are of the order of 1 atm, so the idea gas law is applicable; from this, the continuity equation, and Darcy's law one can show that the square of the gas pressure obeys Laplace's equation,

$$\nabla^2 P^2 = 0 \tag{1}$$

This must be solved with suitable boundary conditions and with a sink term representing the stripping well. The gas velocity is then calculated from Darcy's law,

$$v = -K_D \nabla P \tag{2}$$

Calculation of the soil gas velocities around a vapor stripping well can be done by solving Laplace's equation by the method of images (from electrostatics) or by a numerical relaxation technique (*13*); the relaxation technique gives one greater flexibility in selecting boundary conditions, and this is what is used here. The system is assumed to have axial symmetry, and the soil permeability K_D is assumed to be constant and isotropic. (More general models can readily be constructed, but cannot readily be run on microcomputers such as the IBM PC-AT and its clones; also, data for calculating the model parameters are usually not sufficiently precise to warrant such refinements.) The relationship between gas flow rate (mol/s) and the soil permeability is given by

$$K_D = \frac{QRT}{2\pi \nu r_s(P_a^2 - P_f^2)} \tag{3}$$

where Q is the molar gas flow rate, r_s is the packed radius of the vapor stripping well, P_a is the ambient pressure (about 1 atm), P_f is the pressure at the well head (<1 atm), ν is the voids fraction of the soil, R is the gas constant (8.206×10^{-5} $m^3 \cdot$atm/mol$\cdot$degree, and T is the temperature (degrees K).

The modeling of soil vapor stripping is then done by partitioning the soil to be aerated into a number of small volume elements and carrying out a mass balance on each. It is assumed that Henry's law adequately describes the partitioning of the volatile contaminant between the moving vapor phase and the stationary phase (either interstitial liquid or adsorption sites on solid particles). Use of more elaborate isotherms is quite possible, but to our knowledge the data to support these are not yet available. The set of differential equations for the mass balance on each volume element is then integrated forward in time numerically. The model for field stripping by means of soil vapor stripping well requires the use of two space coordinates, r and z in cylindrical coordinates, and the equations are moderately complex. Let m be the mass of volatile solvent per unit volume at any point in the zone of influence of the well, ν be the soil voids fraction, and w be the soil specific volume of stationary liquid phase. If we assume local equilibrium and Henry's law, then the mass balance for a volume element gives

$$\frac{\partial m}{\partial t} = -\frac{\nabla \cdot (\bar{v} m)}{1 + w/\nu K_H} \tag{4}$$

where K_H is the effective Henry's constant (dimensionless) of the volatile solvent. The equation is approximated by a set of coupled ordinary differential equations, one for each volume element. A cylindrical domain of influence extending from the surface of the soil down to the water table or other impermeable bottom boundary is used. The vapor stripping well is represented by a sink on the z-axis at the specified depth below the surface.

In our earlier work with the model it had become apparent that removal of contaminants from the outer portions of the lower part of the cylindrical zone of influence was the limiting factor in determining the time required for clean up by soil vapor stripping. The thought occurred to us that introduction of passive wells (vent pipes) around the periphery of the zone of influence might markedly increase the rate of clean up by increasing the gas velocities in this relatively stagnant portion of the zone of influence. [This was suggested earlier, actually, in an American Petroleum Institute report (*14*).] In the next section we examine that possibility.

EFFICACY OF PASSIVE VENT WELLS

We assume a cylindrical zone of influence for the vapor stripping well; the notation is indicated in Fig. 1. Cylindrical coordinates are used, and we approximate by assuming axial symmetry. The vacuum well is represented by a sink at $(0,a)$. The desired Laplace's equation is then given by

$$\frac{1}{r}\frac{\partial}{\partial r}\left(r\frac{\partial P^2}{\partial r}\right) + \frac{\partial^2 P^2}{\partial z^2} = 0 \tag{5}$$

We partition this cylindrical volume into a number of annular rings of heights Δz and width Δr; the midpoint of a cross section through the ijth ring is given by

$$r_i = (i - \tfrac{1}{2})\Delta r \tag{6}$$

$$z_j = (j - \tfrac{1}{2})\Delta z \tag{7}$$

In order to include the sink representing the vacuum well, we write

$$P^2 = U - \frac{A}{[r^2 + (z - a)^2]^{1/2}} \tag{8}$$

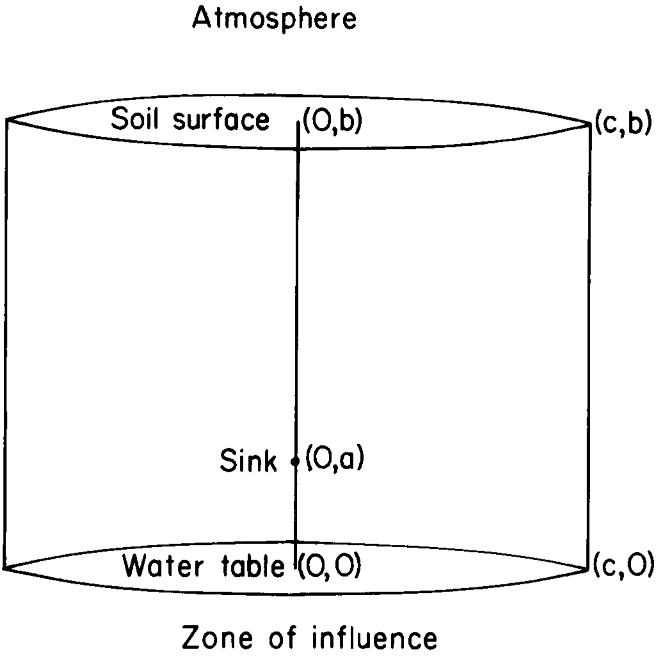

FIG. 1. The zone of influence. The vapor stripping well is represented by a sink at (0,*a*). The presence of peripheral passive vent pipes is represented by requiring that the soil gas pressure be equal to 1 atm on the circumference of the zone of influence. If these are screened only at the bottom, this boundary condition is maintained only for the first meter of the periphery of the zone of influence.

where

$$A = r_s(P_a^2 - P_f^2) \tag{9}$$

r_s = screened radius of well

Here U is a solution of Laplace's equation which is regular at the location of the sink (0,*a*), and which will be chosen to allow P^2 to satisfy the boundary conditions which are desired.

We represent Eq. (5) by means of finite differences, which yields

$$0 = \Delta z(i-1)(-P_{i,j}^2 + P_{i-1,j}^2) + \Delta z \cdot i(-P_{i,j}^2 + P_{i+1,j}^2) + \Delta r(i - \tfrac{1}{2})(P_{i,j+1}^2 - 2P_{i,j}^2 + P_{i,j-1}^2) \tag{10}$$

We shall consider three different sets of boundary conditions. The first corresponds to a vapor stripping well which is in the interior of a hexagonal array of vapor stripping wells; no passive vent wells are present. For this set-up we take the boundary conditions to be

$$P^2(r,b) = 1 \text{ atm}^2 \tag{11}$$

$$\frac{\partial P^2}{\partial r}(c,z) = 0 \tag{12}$$

$$\frac{\partial P^2}{\partial z}(r,0) = 0 \tag{13}$$

Equation (11) gives an ambient pressure of 1 atm at the surface of the soil. Equation (12) gives a no-flow condition through the boundary which the zone of influence shares with the zones of influence of the neighboring vapor stripping wells, approximately. Equation (13) gives a no-flow condition through the bottom of the zone of influence, at which we find the water table or gas-impervious layer.

The second set of boundary conditions corresponds to a vapor stripping well which is surrounded by six passive vent wells which are drilled down to the water table and are screened along their entire length. These yield

$$P^2(r,b) = 1 \text{ atm}^2 \tag{14}$$

$$P^2(c,z) = 1 \text{ atm}^2 \tag{15}$$

$$\frac{\partial P^2}{\partial z}(r,0) = 0 \tag{16}$$

We note that the boundary condition represented by Eq. (15) is approximate.

The third set of boundary conditions corresponds to a vapor stripping well which is surrounded by six passive vent wells which are drilled down to the water table and are screened only along the bottom 1 m of their length; the boundary condition along the periphery of the zone of influence is Eq. (12) if z is greater than 1 m, Eq. (15) if z is less than 1 m.

Let us substitute Eq. (8) into Eq. (10), define

$$f(r,z) = \frac{A}{[r^2 + (z-a)^2]^{1/2}} \tag{17}$$

and note that $f(r,z)$ is itself a solution to Laplace's equation. Solving the equation resulting from the substitution for $U(r_i,z_j) = U_{i,j}$ then yields

$$U_{i,j} = \frac{(i-1)\Delta z U_{i-1,j} + i\Delta z U_{i+1,j} + (i-\frac{1}{2})\Delta r(U_{i,j-1} + U_{i,j+1})}{(2i-1)\Delta z + (2i-1)\Delta r} \tag{18}$$

We set $\Delta z = \Delta r = 1$ m henceforth.

A Taylor's series expansion method described by Gannon (*14*) gives us the equations for the $U_{i,j}$ on the top of the zone of influence; they are

$$U_{i,b} = f_{i,b} + \frac{8}{15}\left[1 + \frac{5}{4}(U_{i,b-1} - f_{i,b-1}) - \frac{3}{8}(U_{i,b-2} - f_{i,b-2})\right] \tag{19}$$

At the bottom of the zone of influence the requirement of zero gas flux through the bottom face of each volume gives

$$\begin{aligned} U_{i,1} = f_{i,1} + \frac{1}{3(i-\frac{1}{2})}&[i(U_{i+1,1} - f_{i+1,1}) + (i-\tfrac{1}{2})(U_{i,2} - f_{i,2}) \\ &+ (i-1)(U_{i-1,1} - f_{i-1,1})] \end{aligned} \tag{20}$$

If no passive vent wells are drilled around the periphery of the zone of influence, Eq. (12) is operative; the requirement of zero gas flux through the outer face of each of the peripheral volume elements then yields

$$\begin{aligned} U_{c,j} = f_{c,j} + \frac{1}{3c-2}&\left[(c-1)(U_{c-1,j} - f_{c-1,j}) + \left(c - \frac{1}{2}\right)\right. \\ &\left.\times (U_{c,j+1} - f_{c,j+1} + U_{c,j-1} - f_{c,j-1})\right] \end{aligned} \tag{21}$$

In similar fashion, one constructs equations for $U_{1,1}$, $U_{1,b}$, $U_{c,j}$, and $U_{c,b}$.

These equations are then solved iteratively for the $U_{i,j}$; for a zone of influence 10 m deep by 20 m in diameter, this takes about 10 min on an MMG-286 microcomputer (an AT clone) with an 80287 math chip running TurboBASIC at 10 MHz. Pressures are calculated from Eq. (22):

$$P_{i,j} = (U_{i,j} - f_{i,j})^{1/2} \tag{22}$$

and the gas velocities are calculated at the faces of the volume elements by finite differences, as illustrated by Eqs. (23) and (24):

$$v_r(i - \tfrac{1}{2},j) = K_D(P_{i-1,j} - P_{i,j}) \tag{23}$$

$$v_z(i,j + \tfrac{1}{2}) = K_D(P_{i,j} - P_{i,j+1}) \tag{24}$$

These velocities are then used in a finite difference representation of Eq. (4) in cylindrical coordinates; this was described in detail in earlier papers (*1*, *2*).

RESULTS, PASSIVE VENT WELLS

The parameters describing the models run are given in Table 1. The airflow rate and wellhead pressure were chosen on the basis of data obtained from a test soil vapor stripping site near Philadelphia. Three sets of runs were made. In the first set, the depth of the water table was 6 m and the depth of the vapor stripping well was 5 m. In the second, the depth of the water table was 8 m and the depth of the stripping well was 6 m. In the third, the depth of the water was 10 m and the depth of the stripping well was 8 m. In each set, three runs were made. The first run in each set simulated a vapor stripping well with no vent pipes around the periphery of the zone of influence. The second run in each set simulated a stripping well, the zone of influence of which is surrounded by passive vent wells extending down to the water table and screened along their entire length. The third run in each set described a stripping well, the zone of influence of which is surrounded by passive vent wells extending to the water table and screened at the bottom for a length of 1 m.

The results of the first set of runs are shown in Fig. 2. Here the $\log_{10}$ of the total mass of violatile contaminant is plotted versus the time. The

TABLE 1
Parameters Used in Modeling Vapor Stripping

Radius of zone of influence	10 m
Screened radius of well	0.12 m
Temperature	12 °C
Soil voids fraction	0.2
Volume fraction of soil liquid	0.2
Gas flow rate	1.0 mol/s (0.0234 m^3/s at 1 atm)
Darcy's constant	0.6206 $m^3/atm \cdot s$
Depth of water table	6, 8, 10 m
Depth of vapor stripping well	5, 6, 8 m
Henry's constant of volatile contaminant	0.001 (dimensionless)

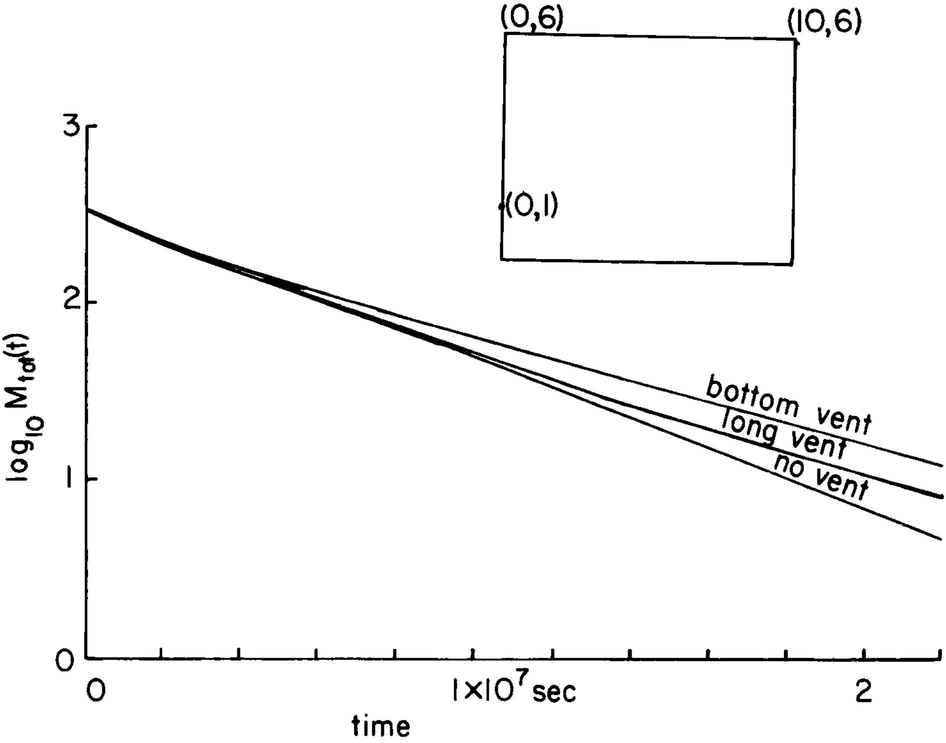

FIG. 2. Plot of $\log_{10} M_{\text{total}}(t)$ versus t. The parameters of the runs are as described in Table 1, and the geometry of the zone of influence is also indicated in the inset to the figure.

differences in the plots are relatively slight, but it is apparent that the removal rate from the zone of influence with no passive vent wells around the periphery is of the order of 10 to 20% greater than are the removal rates from the zones of influence in which passive vent wells are present.

Figure 3 displays the results of the second set of runs for a zone of influence 8 m deep and 10 m in radius. Again we find that the rate of removal of volatile contaminant is greatest for the system in which the zone of influence has no passive vent wells around its periphery. Here the use of passive vent wells may result in decreases in removal rate by as much as 40–50%.

The third set of runs, for a zone of influence 10 m deep and 10 m in radius, gave the results shown in Fig. 4. These runs show the same general

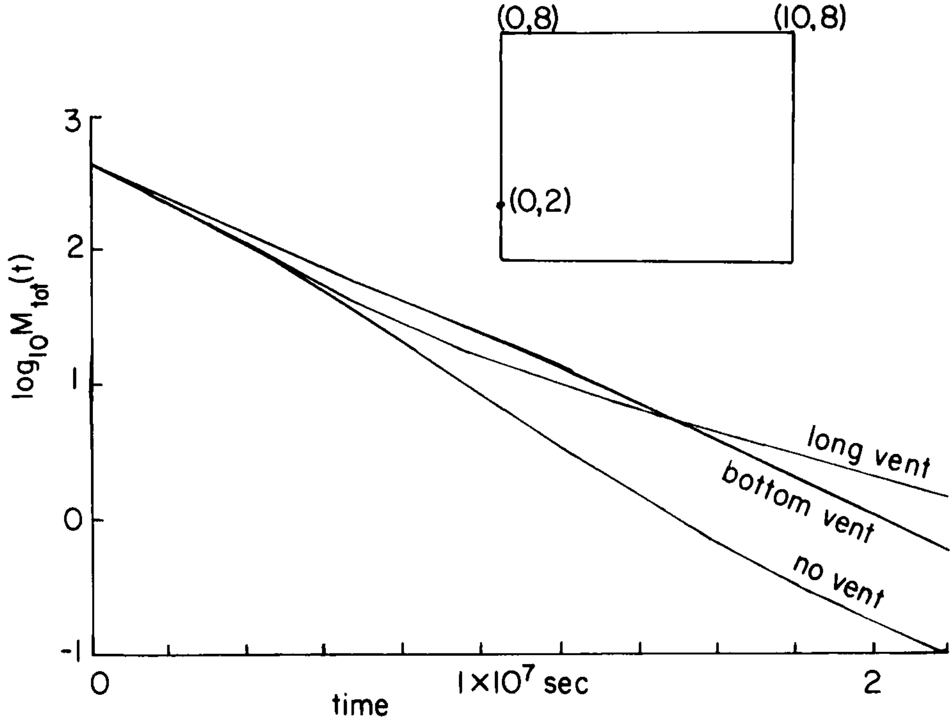

FIG. 3. Plot of $\log_{10} M_{total}(t)$ versus t. Run parameters are given in Table 1; the inset shows the geometry of the zone of influence.

feature that we have seen in the other two sets; the presence of passive vent wells around the periphery of the zone of influence decreases the rate of contaminant removal noticeably.

These results were not what we had expected, so we examined the changing distribution of contaminant within the zone of influence during the course of a simulated vapor stripping run. As the run evolved, it fairly quickly became apparent that the passive vent wells were providing a "short circuit" for the soil gas across the bottom portion of the zone of influence to the vacuum well. Clearance of contaminant from this region was rapid. Clearance of contaminant from a region in the vicinity of the conical surface generated by rotation of a line from the sink at $(0,a)$ to the upper, outer edge of the zone of influence, at (c,b), was greatly decreased, however. This seemed to be responsible for the

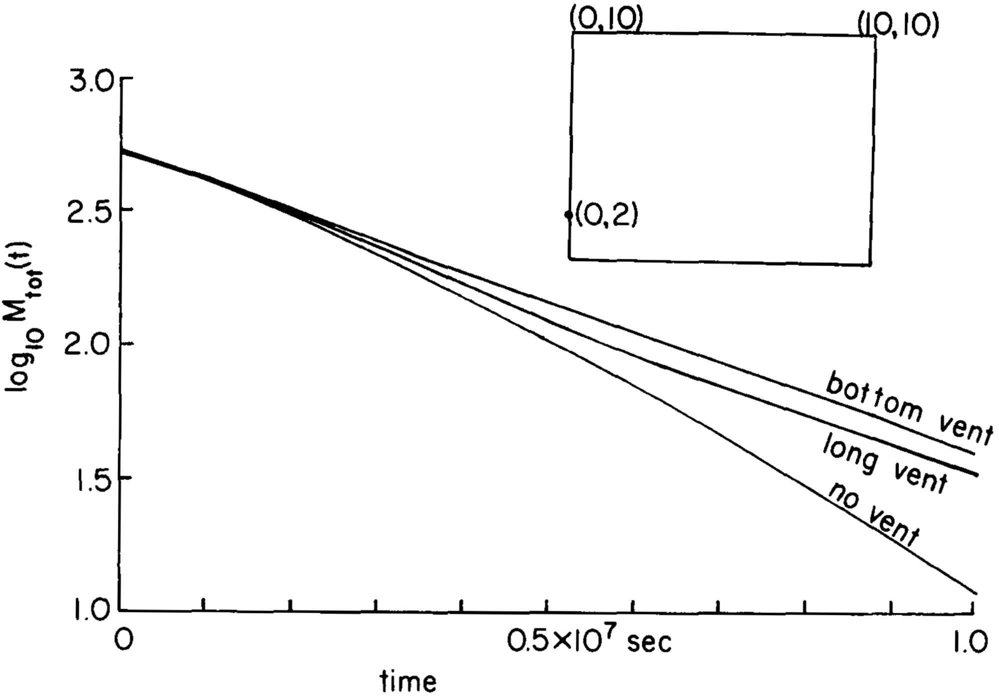

FIG. 4. Plot of $\log_{10} M_{\text{total}}(t)$ versus t. Run parameters are given in Table 1, and the geometry is shown in the inset.

increased removal times found when passive vent pipes were included in the model.

We conclude that, contrary to what intuition might suggest, the use of passive vent wells around the periphery of the zone of influence of a soil vapor stripping well is generally counter-productive. It might be possible to construct geometries for which this is not true, but we expect that these will describe zones of influence the radii of which are very much larger that the depths, and we found earlier (*1*) that such zones of influence make for very inefficient soil vapor stripping.

RECONTAMINATION FROM BELOW THE VADOSE ZONE

One of the questions arising in connection with the design of soil vapor stripping operations is the extent to which recontamination of a vadose zone will occur if this is underlain by either contaminated groundwater or by nonaqueous phase liquid (NAPL). If recontamination is relatively slow, one may carry out soil vapor stripping simultaneously with or even before groundwater pump-and-treat operations and/or removal of NAPL. If recontamination is relatively rapid, then it is necessary to remove the underlying source of contaminant before beginning soil vapor stripping, or at least to have this done well before the soil vapor stripping operation is complete.

In this section we discuss the mathematical modeling of recontamination. The recontamination of the vadose zone by an underlying layer of volatile NAPL is first examined; then we address recontamination from an underlying layer of ground water contaminated with a volatile organic compound (VOC) which in aqueous solution obeys Henry's law.

Recontamination by an Underlying Layer of NAPL

We consider a one-dimensional model for recontamination, as sketched in Fig. 5.

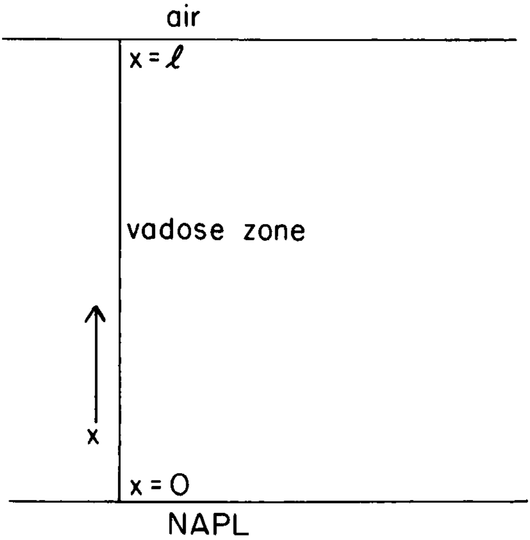

FIG. 5. Geometry of the model for recontamination of the vadose zone by diffusion from underlying NAPL.

Let x = distance above NAPL layer, m
l = thickness of the vadose zone, m
$c(x,t)$ = concentration of contaminant in the vapor phase at point x and time t, kg/m^3
p = total soil voids fraction (gas and liquid), dimensionless
w = soil specific moisture content, dimensionless
K_H = Henry's constant of contaminant, vapor/liquid, dimensionless
P_0 = equilibrium vapor pressure of contaminant, torr
T = ambient temperature, °K
MW = molecular weight of contaminant, kg/mol
D' = diffusion constant of contaminant in the vapor phase, m^2/s
$\nu = p - w$ = soil specific gas volume

Local equilibrium between the liquid and vapor phases is assumed, and diffusion in the liquid phase is assumed to be negligible compared to diffusion in the vapor phase. Then

$$(\nu + wK_H^{-1}) \frac{\partial c}{\partial t} = \nu D' \frac{\partial^2 c}{\partial x^2} \tag{25}$$

which we rewrite as

$$\frac{\partial c}{\partial t} = D \frac{\partial^2 c}{\partial x^2} \tag{26}$$

where

$$D = \frac{D'}{1 + w/\nu K_H} \tag{27}$$

The initial condition for the system we take to be

$$c(x,0) = 0, \qquad 0 < x < l \tag{28}$$

corresponding to an initially uncontaminated vadose zone. The boundary conditions are

$$c(0,t) = c_0 \tag{29}$$

where c_0 is given by

$$c_0 = \frac{P_0 \cdot (\mathrm{MW})}{RT} = \frac{P_0(\mathrm{torr})(\mathrm{MW}) \cdot 1.603 \times 10^{-5}}{T} \tag{30}$$

and

$$c(l,t) = 0 \tag{31}$$

Equation (29) comes from the requirement that the partial pressure of the contaminant at the NAPL layer be the equilibrium vapor pressure of the contaminant. Equation (31) comes from the assumption that air movement maintains essentially a zero concentration of contaminant at the top of the soil.

Equation (26) is solved by separating the variables, as follows. Let

$$c = T(t) \cdot X(x) \tag{32}$$

Then in the usual way

$$\frac{\dot{T}}{T} = \frac{DX''}{X} = -\lambda \tag{33}$$

so

$$T = \exp(-\lambda t) \tag{34}$$

and

$$X'' + \frac{\lambda X}{D} = 0 \tag{35}$$

The steady-state solution to Eq. (26) which satisfies the boundary conditions is

$$c(x,\infty) = c_0(l - x)/l \tag{36}$$

This suggests that we write

$$c(x,t) = c_0 \frac{(l - x)}{l} + \sum_{\lambda} U_\lambda(x) \exp(-\lambda t) \tag{37}$$

The bounary conditions on the U are

$$U_\lambda(0) = 0 \tag{38}$$

$$U_\lambda(l) = 0 \tag{39}$$

and from Eq. (35) we find that

$$U_\lambda'' + \frac{\lambda}{D} U_\lambda = 0 \tag{40}$$

From this we see that

$$U_\lambda = A_\lambda \sin \sqrt{\frac{\lambda}{D}}\, x + B_\lambda \cos \sqrt{\frac{\lambda}{D}}\, x \tag{41}$$

From Eq. (38) it is apparent that $B_\lambda = 0$ for all λ; from Eq. (39), that

$$\sqrt{\frac{\lambda}{D}}\, l = n\pi, \qquad n = 1, 2, 3, \ldots \tag{42}$$

so that

$$\lambda = \frac{Dn^2\pi^2}{l^2} = \lambda_n \tag{43}$$

Then

$$c(x,t) = c_0 \frac{(l-x)}{l} + \sum_{n=1}^{\infty} A_n \sin\left(\frac{n\pi x}{l}\right) \exp\left(-\frac{n^2\pi^2 Dt}{l^2}\right) \tag{44}$$

The initial conditions (Eq. 28) give

$$0 = c_0 \frac{(l-x)}{l} + \sum_{n=1}^{\infty} A_n \sin\left(\frac{n\pi x}{l}\right) \tag{45}$$

so

$$-c_0 \frac{(l-x)}{l} = \sum_{n=1}^{\infty} A_n \sin\left(\frac{n\pi x}{l}\right) \tag{46}$$

Multiply by sin $(m\pi x/l)$ and integrate from 0 to l to get

$$-\frac{c_0}{l}\int_0^l (l-x)\sin\frac{m\pi x}{l}\,dx = 0 + A_m\int_0^l \sin^2\frac{m\pi x}{l}\,dx + 0 \tag{47}$$

This yields

$$A_m = -\frac{2c_0}{m\pi}, \qquad m = 1, 2, 3, \ldots \tag{48}$$

So

$$c(x,t) = c_0\frac{(l-x)}{l} - \frac{2c_0}{\pi}\sum_{n=1}^{\infty}\frac{1}{n}\sin\frac{n\pi x}{l}\exp\left(-\frac{n^2\pi^2 Dt}{l^2}\right) \tag{49}$$

The maximum contaminant flux per unit area from the surface of the soil is given by

$$F_{\max} = \lim_{t\to\infty} - \frac{D\partial c}{\partial x} = Dc_0/l \tag{50}$$

The slowest time constant for the approach to this maximum flux is given by

$$\lambda_1 = \frac{\pi^2 D}{l^2} = \frac{\pi^2 D'}{l^2(1 + w/vK_H)} \tag{51}$$

The flux per unit area of contaminant through the surface is given by

$$F(t) = -\frac{D'\partial c}{\partial x}(l,t) \tag{52}$$

$$= \frac{D'c_0}{l}\left[1 + 2\sum_{n=1}^{\infty}(-1)^n\exp\left(-\frac{n^2\pi^2 Dt}{l^2}\right)\right] \tag{53}$$

It is evident from Eqs. (49), (51), and (53) that the recontamination process can be described in terms of a reduced time $t' = Dt/l^2$, a reduced concentration variable $c' = c(x,t)/c_0$, and a reduced flux $F' = F(t)l/(D'c_0)$. The recontamination process from an underlying layer of NAPL can therefore be completely described by one set of curves in which $c'(x,t)$ is plotted against x for various values of t, and one plot of reduced flux versus t. Such plots are given in Figs. 6 and 7. We see that the time required for significant loss of contaminant to the atmosphere is of the order of λ_1^{-1}, or $l^2(1 + w/\nu K_H)/\pi^2 D'$.

Another relevant quantity in describing recontamination is the total quantity of contaminant which has diffused into the vadose zone. This is given by

$$M(t) = \int_0^l c(x,t) \cdot (\nu + wK_H^{-1}) dx \tag{54}$$

From this we get

$$\frac{M(t)}{\nu + wK_H^{-1}} = \frac{c_0}{l} \int_0^l (l - x) dx - \frac{2c_0}{\pi} \sum_{n=1}^{\infty} \frac{1}{n} \exp\left(-\frac{n^2\pi^2 Dt}{l^2}\right) \cdot \int_0^l \sin\left(\frac{n\pi x}{l}\right) dx\Bigg) \tag{55}$$

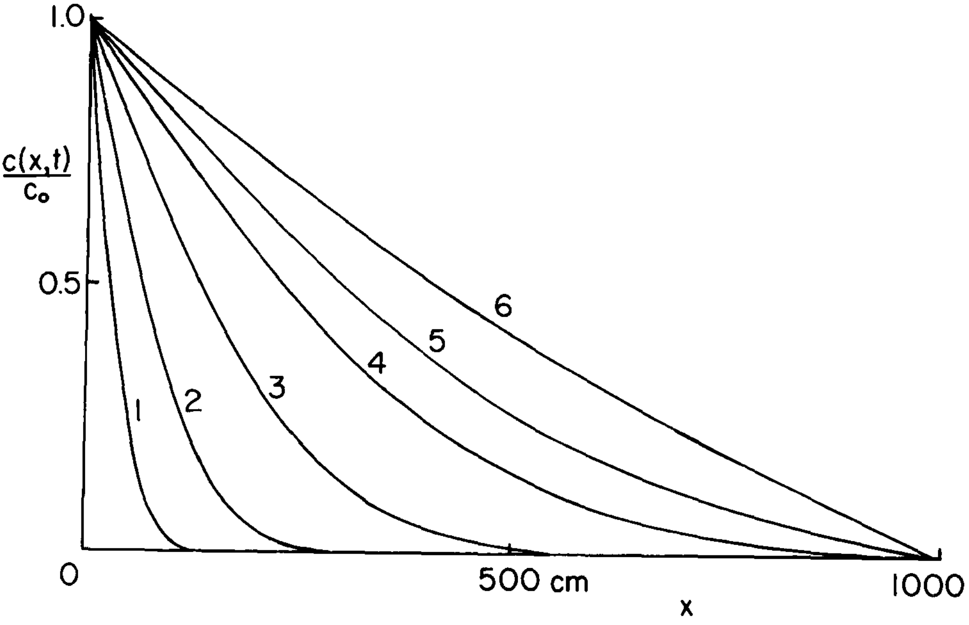

FIG. 6. Plots of $c(x,t)/c_0$ versus x for various values of t, l = 1.0 m; $D = 1 \times 10^{-4}$ m^2/s; t = 1, 5, 20, 60, 100, and 200 × 10^3 s.

$$= \frac{c_0}{l}(l^2 - l^2/2) - \frac{2c_0 l}{\pi^2}\sum_{n=1}^{\infty}\frac{1}{n^2}[1-(-1)^n]\exp\left(-\frac{n^2\pi^2 Dt}{l^2}\right) \tag{56}$$

From this we define a reduced total quantity of contaminant by

$$M'(t) = \frac{2M(t)}{(\nu + wK_{\mathrm{H}}^{-1})} = 1 - \frac{8}{\pi^2}\sum_{m=1}^{\infty}\frac{1}{(2m-1)^2}\exp\left[-\frac{(2m-1)^2\pi^2 Dt}{l^2}\right] \tag{57}$$

A plot of this function is shown in Fig. 8. Unlike the plot of contaminant flux through the soil surface, the total mass of contaminant in the vadose zone initially increases rapidly from zero. This is actually what intuition would suggest, since initially the concentration gradient near the bottom of the vadose zone is very large and therefore drives a large flux from the NAPL layer into the vadose zone. This result indicates that, as one would expect, soil gas composition near the surface of the soil gives a very poor measure of the extent of recontamination from below. This is consistent

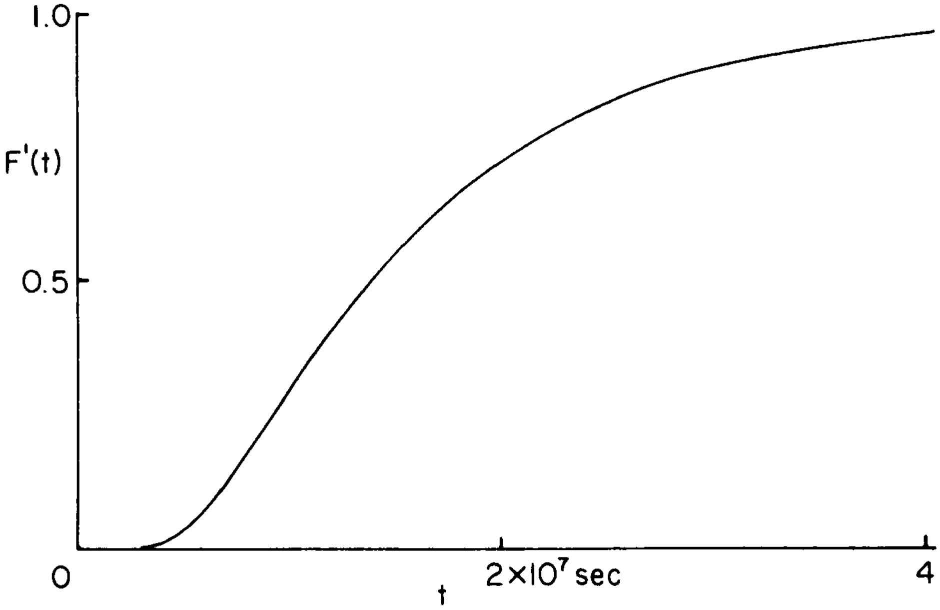

FIG. 7. Plot of reduced contaminant flux through the soil surface, $F'(t)$, versus t. $l = 1.0$ m; $D = 1 \times 10^{-4}$ m^2/s.

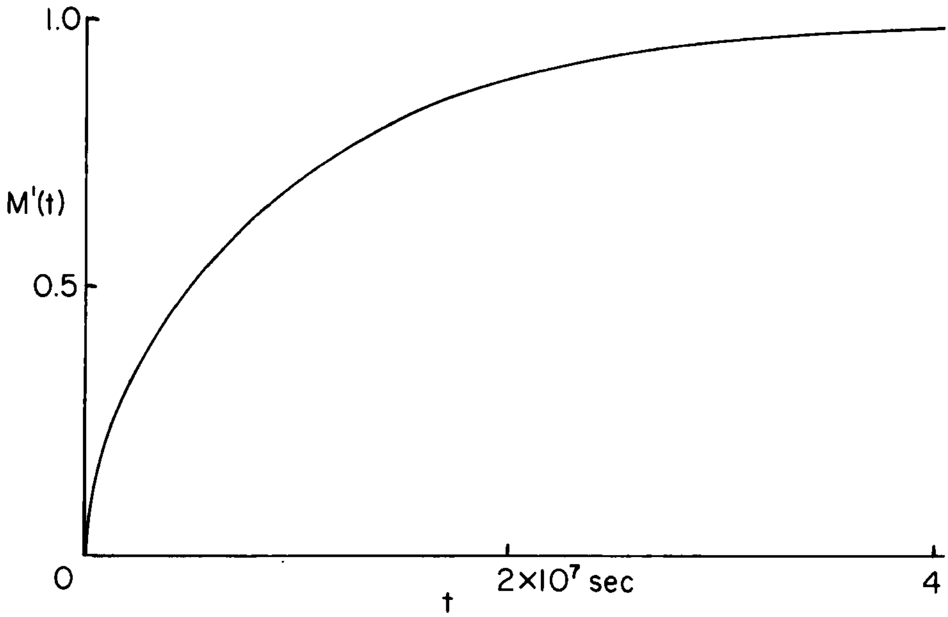

FIG. 8. Plot of reduced contaminant mass in the vadose zone, $M'(t)$, versus t. $l = 1.0$ m; $D = 1 \times 10^{-4}$ m^2/s.

with the series of concentration plots shown in Fig. 6. The speed with which the total mass of contaminant in the vadose zone increases initially also suggests that, unless one is certain that the value of D' of the contaminant in the soil of interest is quite small, one should remove any underlying pools of NAPL before initiating soil vapor stripping. One way of doing this is by evaporating and stripping the NAPL by means of one or more vapor stripping wells screened down near the surface of the NAPL layer. This will be discussed in a later section.

Recontamination of Vapor-Stripped Soil Underlain by Groundwater Containing Dissolved VOC

Again we consider a one-dimensional model for recontamination, this time as sketched in Fig. 9. If the flow of groundwater is sufficient to maintain a nearly constant concentration of contaminant in the zone of saturation, we can use a minor modification of our previous result. In Eq.

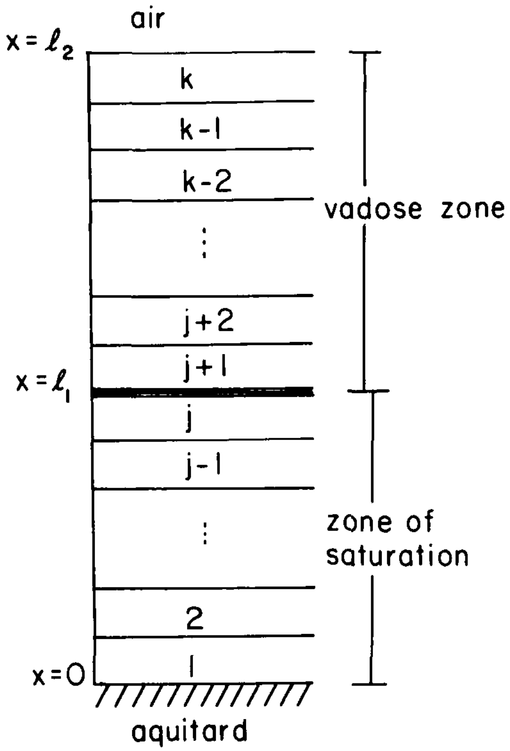

FIG. 9. Geometry of the model for recontamination of the vadose zone by diffusion from an underlying zone of saturation contaminated with VOC.

(30) we merely replace the vapor pressure of the neat contaminant by the equilibrium vapor pressure of the contaminant above a solution having the composition of the groundwater and at the ambient soil temperature.

If the contaminant concentration in the upper layer of the groundwater is significantly depleted by evaporative losses to the vadose zone, the analysis is somewhat more lengthy. We first use an eigenvalue approach to estimate the time constants involved, after which we examine the results obtained with this model by numerical integration. Lastly, the eigenvalue-eigenfunction and numerical integration methods are used to examine the long-time pseudo-steady-state behavior of the system.

Let D_1 = contaminant diffusion constant in the zone of saturation, cm^2/s

D_2' = contaminant diffusion constant in the vapor phase in the vadose zone, cm^2/s
l_1 = thickness of the zone of saturation, cm
$l_2 - l_1$ = thickness of the vadose zone, cm
$p_{1,2}$ = soil porosity, both zones
w_2 = specific moisture content, vadose zone
$v_2 = p_2 - w_2$ = specific gas volume in the vadose zone
K_H = Henry's constant of contaminant in aqueous solution
$D_2 = v_2 D_2'/(v_2 + w_2 K_H^{-1})$
$c(x,t)$ = liquid phase contaminant concentration in the zone of saturation, $0 < x < l_1$
= vapor phase contaminant concentration, $l_1 < x < l_2$

We take as the initial conditions for the problem

$$\begin{aligned} c(x,0) &= c_2, \quad 0 < x < l_1 \\ c(x,0) &= 0, \quad l_1 < x < l_2 \end{aligned} \tag{58}$$

The boundary conditions are

$$\lim_{\delta \to 0^+} c(l_1 - \delta,t) = K_H^{-1} \lim_{\delta \to 0^+} c(l_1 + \delta,t) \tag{59}$$

$$\lim_{\delta \to 0^+} p_1 D_1 \frac{\partial c}{\partial x}(l_1 - \delta,t) = \lim_{\delta \to 0^+} (p_2 - w_2) D_2 \frac{\partial c}{\partial x}(l_1 + \delta,t) \tag{60}$$

$$\frac{\partial c}{\partial x}(0,t) = 0 \tag{61}$$

$$c(l_2,t) = 0 \tag{62}$$

The first boundary condition comes from Henry's law and the assumption of local equilibrium at the boundary between the vadose zone and the zone of saturation. The second comes from the requirement that the contaminant flux be conserved at the boundary between the two zones. The third comes from the requirement that there be no flux through the impermeable boundary underlying the zone of saturation. The fourth represents the assumption that air movement above the soil surface maintains essentially a zero concentration of VOC at the soil surface.

In Region I the diffusion equation is

$$\frac{\partial c}{\partial t} = D_1 \frac{\partial^2 c}{\partial x^2} \tag{63}$$

A solution to this equation which satisfies Eq. (61) is

$$c(x,t) = \sum_{\lambda} A_{\lambda} \cos \sqrt{\frac{\lambda}{D_1}}\, x \exp(-\lambda t) \tag{64}$$

In region II the diffusion equation is

$$(\nu_2 + w_2 K_{\mathrm{H}}^{-1}) \frac{\partial c}{\partial t} = \nu_2 D_2' \frac{\partial^2 c}{\partial x^2}$$

which we rewrite as

$$\frac{\partial c}{\partial t} = D_2 \frac{\partial^2 c}{\partial x^2} \tag{65}$$

Separation of variables then yields

$$c(x,t) = \sum_{\lambda} \left[B_{\lambda} \sin \sqrt{\frac{\lambda}{D_2}}\, x + C_{\lambda} \cos \sqrt{\frac{\lambda}{D_2}}\, x \right] \exp(-\lambda t) \tag{66}$$

Equations (59), (60), and (62) then yield

$$A_{\lambda} \cos \sqrt{\frac{\lambda}{D_1}}\, l_1 = K_{\mathrm{H}}^{-1} \left[B_{\lambda} \sin \sqrt{\frac{\lambda}{D_2}}\, l_1 + C_{\lambda} \cos \sqrt{\frac{\lambda}{D_2}}\, l_1 \right] \tag{67}$$

$$-p_1 \sqrt{D_1 \lambda}\, A_{\lambda} \sin \sqrt{\frac{\lambda}{D_1}}\, l_1 = \nu_2 \sqrt{D_2 \lambda} \left[B_{\lambda} \cos \sqrt{\frac{\lambda}{D_2}}\, l_1 - C_{\lambda} \sin \sqrt{\frac{\lambda}{D_2}}\, l_1 \right] \tag{68}$$

$$B_{\lambda} \sin \sqrt{\frac{\lambda}{D_2}}\, l_2 + C_{\lambda} \cos \sqrt{\frac{\lambda}{D_2}}\, l_2 = 0 \tag{69}$$

To have nonzero values for A_{λ}, B_{λ}, and C_{λ}, the determinant of the coefficients in these equations must vanish. This gives

$$\begin{vmatrix} 0 & \sin\sqrt{\frac{\lambda}{D_2}}\,l_2 & \cos\sqrt{\frac{\lambda}{D_2}}\,l_2 \\ -\cos\sqrt{\frac{\lambda}{D_1}}\,l_1 & K_H^{-1}\sin\sqrt{\frac{\lambda}{D_2}}\,l_1 & K_H^{-1}\cos\sqrt{\frac{\lambda}{D_2}}\,l_1 \\ p_1\sqrt{D_1}\sin\sqrt{\frac{\lambda}{D_1}}\,l_1 & \nu_2\sqrt{D_2}\cos\sqrt{\frac{\lambda}{D_2}}\,l_1 & -\nu_2\sqrt{D_2}\sin\sqrt{\frac{\lambda}{D_2}}\,l_1 \end{vmatrix} = 0 \qquad (70)$$

Expansion of the determinant and use of some trigonometric identities then yield

$$\frac{\nu_2}{p_1}K_H\sqrt{\frac{D_2}{D_1}} = \tan\left(\sqrt{\frac{\lambda}{D_1}}\,l_1\right)\tan\left(\sqrt{\frac{\lambda}{D_2}}(l_2 - l_1)\right) \qquad (71)$$

The roots of Eq. (72), $\lambda_1, \lambda_2, \ldots$, can then be used to calculate the B_λ and C_λ in terms of the A_λ, giving the eigenfunctions of the problem. The orthogonality of the normalized eigenfunctions can then be used, together with the initial conditions, to calculate the A_λ, yielding an eigenfunction expansion of $c(x,t)$. The eigenvalues are also the time constants for the decay of the system toward equilibrium, at which $c(x,\infty) = 0$, $0 < x < l_2$.

The complexity of these calculations pushed us to attack this diffusion problem by another route—direct numerical integration. This was done as follows.

The domain of interest is partitioned up as indicated in Fig. 9. We let

$$c_i(t) = c[(i - \tfrac{1}{2})\Delta x, t] \qquad (72)$$

and approximate the diffusion equation over this finite set of points as a set of ordinary differential equations. We use, with minor modification, the notation of the last section. Recall that

$$\frac{\nu_2 D_2'}{\nu_2 + w_2 K_H^{-1}} = D_2 \qquad (73)$$

The diffusion equation to be represented is given in Region II by

$$\frac{\partial c}{\partial t} = D_2 \frac{\partial^2 c}{\partial x^2} \tag{74}$$

where c is the contaminant concentration in the vapor phase. In Region I,

$$\frac{\partial c}{\partial t} = D_1 \frac{\partial^2 c}{\partial x^2} \tag{75}$$

The discrete representation of the partial differential equation is as follows. At the top compartment

$$\frac{\partial c_k}{\partial t} = \frac{D_2}{\Delta x^2}(c_{k-1} - 2c_k) \tag{76}$$

due to the boundary condition specified by Eq. (62). At the bottom compartment,

$$\frac{\partial c_1}{\partial t} = \frac{D_1}{\Delta x^2}(c_2 - c_1) \tag{77}$$

from Eq. (61). The boundary conditions at the boundary between the vadose zone and the zone of saturation are

$$K_H c^-_{j+1/2} = c^+_{j+1/2} \tag{78}$$

from Henry's law, and

$$p_1 \frac{D_1(c_j - c^-_{j+1/2})}{\Delta x/2} = \nu_2 \frac{D'_2(c^+_{j+1/2} - c_{j+1})}{\Delta x/2} \tag{79}$$

from the requirement of conservation of flux. Then

$$p_1 D_1 c_j - p_1 D_1 c^-_{j+1/2} = \nu_2 D'_2 c^+_{j+1/2} - \nu_2 D'_2 c_{j+1} \tag{80}$$

Substitute Eq. (78) into Eq. (80) to get, after simplifying and solving for $c^-_{j+1/2}$,

$$c^-_{j+1/2} = p_1 \frac{D_1 c_j + \nu_2 D'_2 c_{j+1}}{p_1 D_1 + \nu_2 D'_2 K_H} \tag{81}$$

and (from Eqs. 78 and 81),

$$c_{j+1/2}^{+} = K_H \frac{(p_1 D_1 c_j + \nu_2 D_2' c_{j+1})}{p_1 D_1 + \nu_2 D_2' K_H} \tag{82}$$

We are now in position to write mass balance equations for the jth and (j + 1)th compartments, which are on either side of the boundary between the zone of saturation and the vadose zone. For the jth compartment we have

$$p_1 \frac{\partial c_j}{\partial t} \Delta x = p_1 D_1 \left[\frac{c_{j-1} - c_j}{\Delta x} + \frac{c_{j+1/2}^{-} - c_j}{\Delta x/2} \right] \tag{83}$$

Substitution of Eq. (81) and simplification then yields

$$\frac{\partial c_j}{\partial t} = \frac{D_1}{\Delta x_2} \left[c_{j-1} - 3c_j + \frac{2p_1 D_1 c_j + \nu_2 D_2' c_{j+1}}{p_1 D_1 + \nu_2 D_2' K_H} \right] \tag{84}$$

For the (j + 1)th compartment

$$(\nu_2 + w_2 K_H^{-1}) \frac{\partial c_{j+1}}{\partial t} \Delta x = \nu_2 D_2' \left[\frac{c_{j-2} - c_{j+1}}{\Delta x} + \frac{c_{j+1/2}^{+} - c_{j+1}}{\Delta x/2} \right] \tag{85}$$

Substitution of Eqs. (73) and (82) and simplification gives

$$\frac{\partial c_{j+1}}{\partial t} = \frac{D_2}{\Delta x^2} \left[c_{j+2} - 3c_{j+1} + 2K_H \frac{(p_1 D_1 c_j + \nu_2 D_2' c_{j+1})}{p_1 D_1 + \nu_2 D_2' K_H} \right] \tag{86}$$

In the interiors of Regions I and II the diffusion equation is represented by

$$\frac{\partial c_i}{\partial t} = \frac{D_1}{\Delta x^2} (c_{i+1} - 2c_i + c_{i-1}), \qquad i = 2, 3, \ldots, j - 1 \tag{87}$$

and

$$\frac{\partial c_i}{\partial t} = \frac{D_2}{\Delta x^2} (c_{i+1} - 2c_i + c_{i-1}), \qquad i = j + 2, j + 3, \ldots, k - 1 \tag{88}$$

These differential equations (Eqs. 76, 77, 84, 86, 87, and 88) and the initial conditions

$$c_i(0) = c_0, \qquad 1 \leqslant i \leqslant j \tag{89}$$

$$c_i(0) = 0, \qquad j + 1 \leqslant i \leqslant k \tag{90}$$

completely specify the problem. A predictor-corrector method was used to integrate the equations forward in time on an MMG 286 microcomputer (an IBM AT clone) running at 10 MHz. The computer program was written in BASICA and compiled; a typical run (such as that shown in Figs. 6 and 7) took about half an hour.

The parameters used for the run plotted in Figs. 10 and 11 are listed in Table 2. These parameters are *not* based on experimental data from any site, and the results should not be regarded as quantitatively significant; the purpose of the runs made was to test the mathematical method and the program. Still, one can draw some conclusions about the behavior of this recontamination process.

First, contaminant diffusion constants in the vapor phase are typically more than an order of magnitude larger than they are in the aqueous

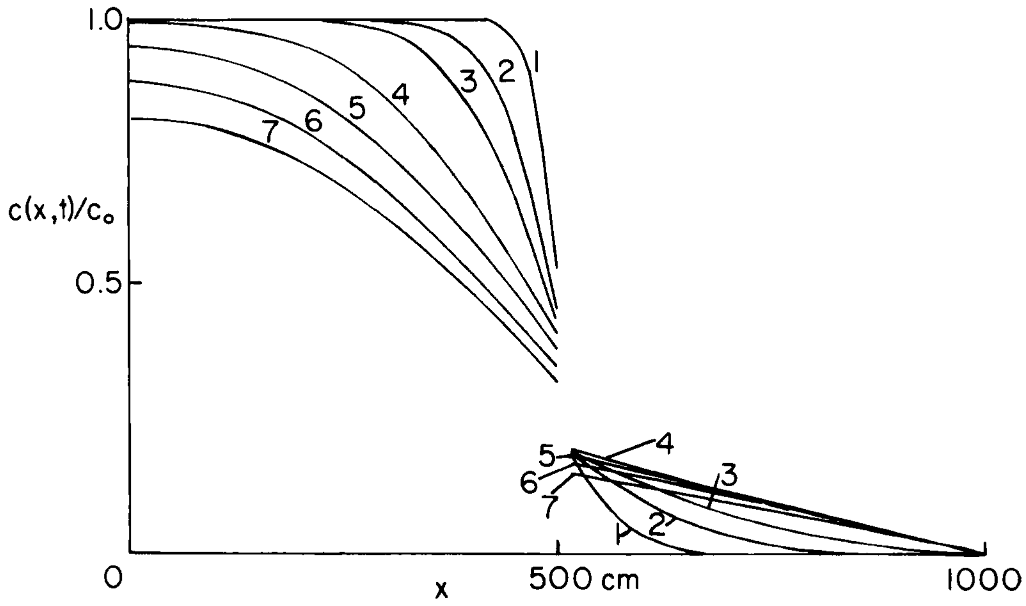

FIG. 10. Contaminant concentration profiles in the zone of saturation and the vadose zone at various times after diffusive transport is initiated. The parameters for the run are given in Table 2.

TABLE 2
Parameters for the Run Plotted in Figs. 10 and 11

l_1	500 cm
l_2	1000 cm
D_1	1 cm^2/s
D_2	3 cm^2/s
Soil voids fraction, both zones	0.4
Volume fraction of soil liquid in the vadose zone	0.2
Contaminant Henry's constant	0.5
Number of compartments in model	30
dt	10 s

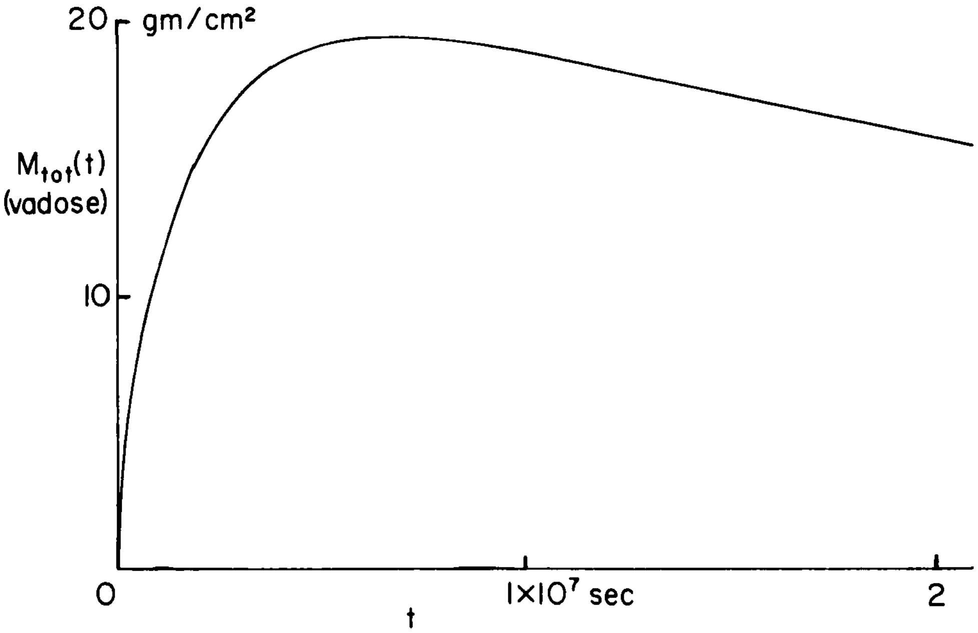

FIG. 11. Total contaminant mass in the vadose zone versus time. Run parameters are given in Table 2.

phase. We therefore expect to see a comparatively rapid development of a diffusion steady state across the vadose zone, in which the concentration varies linearly with depth below the surface. The time required for this should be of the order of $(l_2 - l_1)^2/D_2$. Second, the decay time for decrease in contaminant total mass by diffusion losses should be of the order of l_1^2/D_1, the factor controlling diffusion through the zone of saturation. Last, we expect that the initial rate of recontamination of the vadose zone from below will always be relatively rapid because of the large concentration gradient initially present near the bottom of the vadose zone.

We next provide a simplified treatment which assumes that $D_2 \gg D_1$, so that a pseudosteady state is established comparatively quickly in the vadose zone on the time scale required for depletion of the contaminant from the zone of saturation.

In Region II under pseudosteady-state conditions,

$$c^+ = c^+(l_1) \cdot \frac{l_2 - x}{l_2 - l_1}, \qquad \frac{\partial c^+}{\partial x} = -\frac{c^+(l_1)}{l_2 - l_1} \tag{91}$$

At the boundary between I and II

$$c^+(l_1) = K_H c^-(l_1) \tag{92}$$

from Henry's law, and

$$p_1 D_1 \frac{\partial c^-}{\partial x}(l_1) = \nu_2 D_2' \frac{\partial c^+}{\partial x}(l_1) \tag{93}$$

from conservation of flux at the boundary. Then

$$p_1 D_1 \frac{\partial c^-}{\partial x}(l_1) = \nu_2 D_2'\left(-\frac{c^+(l_1)}{l_2 - l_1}\right) \tag{94}$$

Substitution of Eq. (68) into Eq. (70) then gives

$$p_1 D_1 \frac{\partial c^-}{\partial x}(l_1) = \nu_2 D_2' \cdot \left[-K_H \frac{c^-(l_1)}{l_2 - l_1}\right] \tag{95}$$

Evidently the diffusion problem in Regions I and II has been reduced to a diffusion problem in Region I alone, with boundary conditions

$$\frac{\partial c}{\partial x}(0,t) = 0 \tag{96}$$

and

$$\frac{\partial c}{\partial x}(l_1,t) = -\frac{\nu_2 D_2' K_H}{p_1 D_1 (l_2 - l_1)} c(l_1,t) \tag{97}$$

Recall that a solution of the diffusion equation satisfying the first boundary condition is

$$c(x,t) = \sum_{\lambda} A_\lambda \cos\left(\sqrt{\frac{\lambda}{D_1}}x\right) \exp(-\lambda t) \tag{98}$$

From the second boundary condition (Eq. 97) we get

$$\sqrt{\frac{\lambda}{D_1}} \sin \sqrt{\frac{\lambda}{D_1}} l_1 = -\frac{\nu_2 D_2' K_H}{p_1 D_1 (l_2 - l_1)} \cos \sqrt{\frac{\lambda}{D_1}} l_1 \tag{99}$$

so that the eigenvalues of the system are given by

$$\tan x = -\frac{1}{x}\frac{\nu_2 D_2' K_H l_1}{p_1 D_1 (l_2 - l_1)} \tag{100}$$

where

$$x = \sqrt{\frac{\lambda}{D_1}} l_1 \tag{101}$$

The reciprocal of the least positive value of λ is then the longest time constant associated with the loss of contaminant from the zone of saturation.

More detailed information about the case where one has pseudosteady-state diffusion in the vadose zone is most readily obtained by numerical integration. Generally, in Region I (the zone of saturation) one has

$$\frac{\partial c_i}{\partial t} = \frac{D_1}{\Delta x^2}(c_{i+1} - 2c_i + c_{i-1}) \tag{102}$$

At the bottom of Region I,

$$\frac{\partial c_1}{\partial t} = \frac{D_1}{\Delta x^2}(c_2 - c_1) \tag{103}$$

At the boundary between Region I and Region II, Henry's law gives

$$K_H c_{j+1/2}^- = c_{j+1/2}^+ \tag{104}$$

Flux conservation and the assumption of a pseudosteady-state in Region II give

$$p_1 D_1 \frac{c_{j+1/2}^- - c_j}{\Delta x/2} = \nu_2 D_2' \left(- \frac{c_{j+1/2}^+}{l_2 - l_1} \right) \tag{105}$$

Equations (80) and (81) yield

$$c_{j+1/2}^- = \frac{c_j}{1 + \dfrac{\Delta x \nu_2 D_2' K_H}{2 p_1 D_1 (l_2 - l_1)}} \tag{106}$$

A material balance for the slab at the top of Region I then gives

$$\frac{\partial c_i}{\partial t} = \frac{D_1}{\Delta x^2} \left[c_{j-1} - \left(3 - \frac{2}{1 + \dfrac{\Delta x \nu_2 D_2' K_H}{2 p_1 D_1 (l_2 - l_1)}} \right) c_j \right] \tag{107}$$

Equations (102), (103), and (107) are then integrated forward in time, as before, with Eq. (89) providing the initial conditions.

The standard parameters used for making runs with the pseudosteady-state model are given in Table 3. Figure 12 shows three concentration profiles in the zone of saturation at different times during the course of a run simulating diffusion from the zone of saturation. The presence of the vadose zone with its associated resistance to diffusion gives a nonzero contaminant concentration at the top of the zone of saturation, as expected, and the impermeable boundary at the bottom of the zone of saturation is responsible for the zero slope of the plots on the left-hand side.

In Fig. 13 we see plots of the total mass of contaminant in the zone of saturation versus time for three different thicknesses of the vadose zone—100, 500, and 1000 cm. Increasing thickness of the vadose zone results in an increased resistance to diffusive transport from the zone of saturation to the atmosphere, despite the fact that the diffusion constant of the contaminant in the vadose zone is taken to be ten times larger than its diffusion constant in the zone of saturation.

TABLE 3
Parameters for the Run Plotted in Fig. 12

l_1	500 cm
l_2	1000 cm
D_1	1 cm^2/s
D_2	10 cm^2/s
Soil voids fraction, both zones	0.4
Volume fraction of soil liquid in the vadose zone	0.2
Contamination Henry's constant	0.5
Number of compartments in model	30
dt	50 s
Times (top to bottom)	2, 5, and 20 × 10^7 s

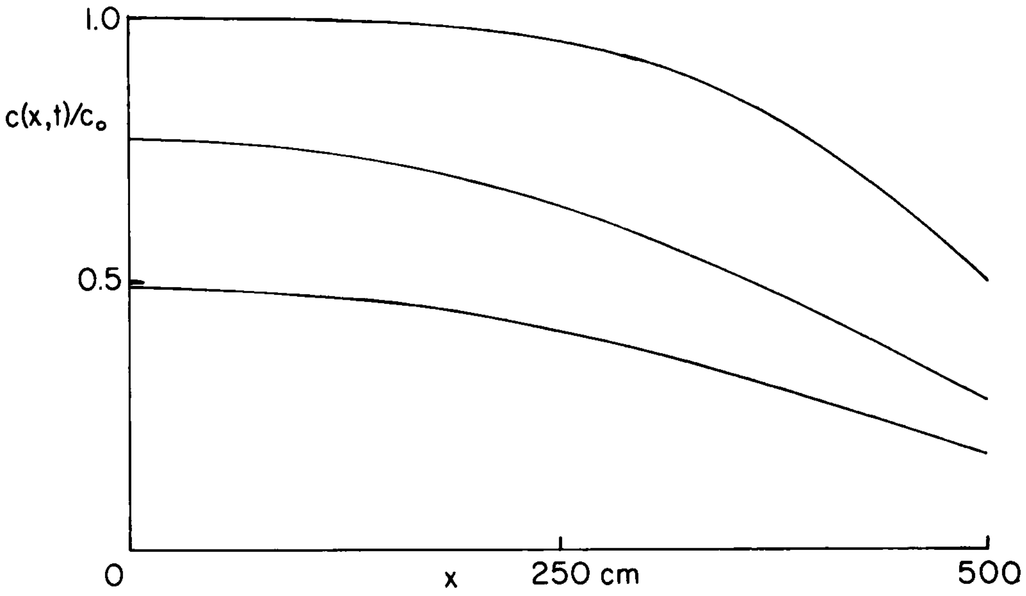

FIG. 12. Contaminant profiles in the zone of saturation at various times after diffusive transport is initiated. These profiles are calculated with the pseudo-steady-state model. Run parameters are given in Table 3.

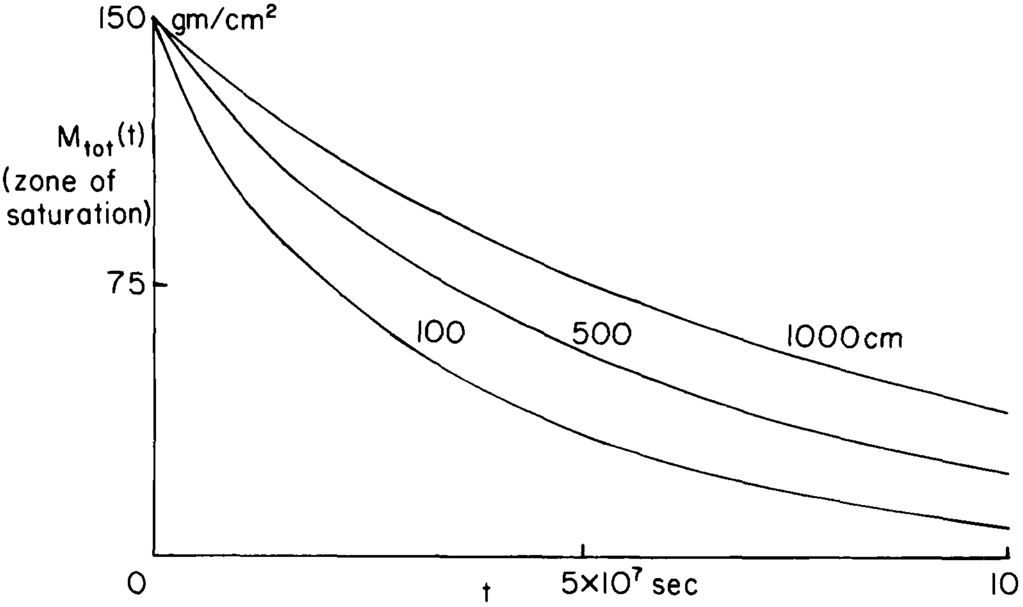

FIG. 13. Total contaminant mass in the zone of saturation versus time. $l_2 - l_1 = 0.1, 0.5$, and 1.0 m (bottom to top). The pseudo-steady-state model was used to calculate these curves.

We conclude that one-dimensional models for diffusive transport from either an underlying NAPL layer or a contaminated zone of saturation are readily constructed and yield results which are in agreement with physical intuition. The utility of the models in any particular case depends, of course, on the availability of experimentally determined diffusion constants, porosities, moisture contents, and effective Henry's constants. The models do suggest that recontamination of the lower portions of the vadose zone by diffusion from underlying NAPL pools and/or ground water contaminated with VOCs may well occur if these are not cleaned up well before soil vapor stripping operations are complete.

REMOVAL OF UNDERLYING NAPL

A point that arises in connection with soil vapor stripping is the extent to which it can remove light nonaqueous phase liquid (LNAPL) floating on top of the water table, and dense nonaqueous phase liquid (DNAPL) either trapped by surface tension effects on top of the water table or held above a soil or rock layer of quite low permeability. If NAPL is present, mass transport from the nonaqueous phase must involve a diffusion step before advective transport by the moving gas becomes possible. The utility of soil vapor stripping would be markedly increased if it could be shown that the technique could be used economically for the removal of NAPL underlying the vadose zone. We address this matter here.

The procedure to be followed here is quite similar to that used in our first paper (*1*); we therefore merely sketch material that was covered in detail in the earlier paper. The calculation of the soil gas velocity field around a stripping well such as that diagrammed in Fig. 14 is done exactly as described earlier (*1*, *2*); the pressure obeys

$$\nabla^2 P^2 = 0 \tag{108}$$

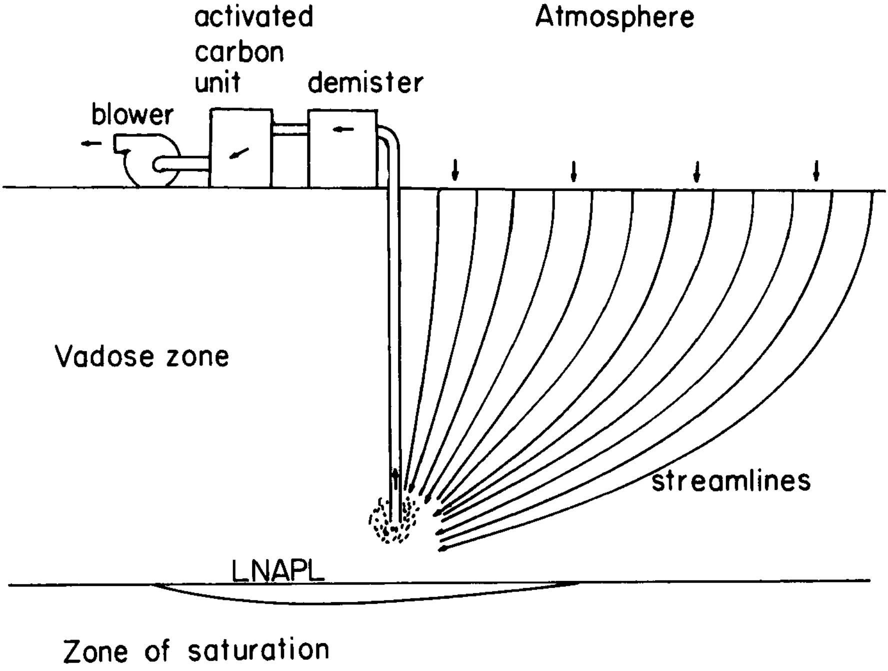

FIG. 14. A sketch of the model used for LNAPL vapor stripping.

and the velocity is calculated by Darcy's law,

$$\bar{v} = -K_{\mathrm{D}}\nabla P \tag{109}$$

Cylindrical symmetry is assumed; the boundary conditions are

$$P = 1 \text{ atm} \tag{110}$$

on the top of the zone of influence,

$$\partial P/\partial z = 0 \tag{111}$$

on the bottom of the zone of influence, and

$$\partial P/\partial r = 0 \tag{112}$$

on the side of the zone of influence. A source term is placed on the axis of the cylindrical zone of influence to represent the well. The details of the calculations have been described previously; actually, velocity fields from these papers were used in our present work.

Mass balance on a volume element in the zone of influence gives

$$\partial m/\partial t = -\nu\nabla \cdot (\bar{v}c^{v}) + \nabla \cdot D\nabla c^{v} \tag{113}$$

Here c^v = vapor concentration of contaminant, kg/m^3
c^l = effective liquid phase concentration of contaminant, kg/m^3
ν = voids fraction in the soil, dimensionless
w = specific volume of water in the soil, dimensionless
m = mass of contaminant per unit volume of soil, kg/m^3
$\bar{v}$ = soil gas velocity, assumed independent of time, m/s
D = dispersion tensor, m^2/s

We assume that c^v and c^l are related by Henry's law, so

$$c^{v} = K_{\mathrm{H}}c^{l} \tag{114}$$

where K_{H} is the effective Henry's constant for the contaminant in the soil liquid phase present in the vadose zone. Then

$$m = \nu c^{v} + wc^{l} \tag{115}$$

which, with Eq. (7), then yields

$$c^v = \frac{m}{\text{v} + wK_{\mathrm{H}}^{-1}} \tag{116}$$

and allows us to write Eq. (113) as

$$\frac{\partial m}{\partial t} = \frac{-\text{v}}{\text{v} + wK_{\mathrm{H}}^{-1}} \nabla \cdot (\bar{v}m) + \frac{D}{\text{v} + wK_{\mathrm{H}}^{-1}} \nabla^2 m \tag{117}$$

(Here we have also assumed that the dispersion constant is isotropic and independent of position.)

The cylindrical symmetry of the model suggests that Eq. (117) be written in cylindrical coordinates

$$\frac{\partial m}{\partial t} = \frac{-\text{v}}{\text{v} + wK_{\mathrm{H}}^{-1}} \left[\frac{1}{r}\frac{\partial}{\partial r}(rv_r m) + \frac{\partial}{\partial z}(v_z m)\right] + \frac{D}{\text{v} + wK_{\mathrm{H}}^{-1}} \left[\frac{1}{r}\frac{\partial m}{\partial r} + \frac{\partial^2 m}{\partial r^2} + \frac{\partial^2 m}{\partial z^2}\right] \tag{118}$$

The boundary conditions are as follows. At the cylindrical periphery of the zone of influence, $v_r = 0$, and we eliminate the diffusion term by virtue of the fact that the presence of surrounding wells will result in $\partial m/\partial r = 0$ at this boundary to a good approximation. On the top of the zone of influence we assume that the air coming into the soil is free from contamination and that we can neglect diffusive losses across this boundary. On the axis of the zone of influence, $v_r = 0$ except at the sink, and $\partial m/\partial r = 0$, so radial diffusion can be dropped. These are all boundary conditions which have been used in our previous calculations.

The boundary condition at the bottom of the zone of influence we take to be

$$m(r,0,t) = (\text{v} + wK_{\mathrm{H}}^{-1})c_0^v \tag{119}$$

where c_0^v is the equilibrium vapor concentration of the NAPL at the ambient soil temperature. This is given in terms of the vapor pressure of the NAPL by

$$c_0^v(\text{g/mL}) = \frac{P(\text{torr}) \times (\text{MW}) \times 1.603 \times 10^{-5}}{T(^\circ\text{K})} \tag{120}$$

We assume that we can neglect the diffusion term in Eq. (118) except for the fact that it generates a source term along the bottom of the zone of influence, where $v_z = 0$. Along this boundary we need to consider diffusion in the vertical direction only, since here $v_r \neq 0$, and we can safely assume that radial movement of contaminant will be dominated by advection.

We are now in position to examine the effect of this bottom boundary condition on the discrete set of ordinary differential equations which are to approximate the partial differential equation, Eq. (118). Let

$$m_{ij}(t) = m[(i - \tfrac{1}{2})\Delta r, (j - \tfrac{1}{2})\Delta z, t] \qquad (121)$$

where $m_{ij}(t)$ is the bulk concentration in the ijth volume element, an annular ring of inner radius $(i - 1)\Delta r$, outer radius $i\Delta r$, and thickness Δz. Then all the equations for $\partial m_{ij}(t)/\partial t$ will be exactly as in I, except that we will have additional terms

$$\left(\frac{\partial m_{i,1}}{\partial t}\right)^{\text{diff}}, \qquad i = 1, 2, \ldots, n_r$$

for the volume elements covering the bottom surface of the zone of influence.

The diffusion terms are calculated as follows. The areas of the four surfaces of the ijth volume element are given by

$$\text{areas of upper and lower surfaces} = 2\pi(2i - 1)(\Delta r)^2 \qquad (122)$$

$$\text{area of inner surface} = 2\pi(i - 1)\Delta r\Delta z \qquad (123)$$

$$\text{area of outer surface} = 2\pi i\Delta r\Delta z \qquad (124)$$

The z-component of the concentration gradient at the bottom of the zone of influence can be approximated by

$$\left(\frac{\partial m}{\partial z}\right)^{\text{diff}}_{i,1} = \frac{[m(i - \tfrac{1}{2})\Delta r^{1/2}\Delta z] - m[(i - \tfrac{1}{2})\Delta r0]}{\Delta z/2} \qquad (125)$$

From Eq. (119), this can be written as

$$\left(\frac{\partial m}{\partial z}\right)^{\text{diff}}_{i,1} = \frac{2[m(i,1) - (\nu + wK_{\mathrm{H}}^{-1})c_0^{\upsilon}]}{\Delta z} \qquad (126)$$

Lastly, a mass balance for an element on the bottom of the zone of influence then gives

$$\frac{\partial m_{i,1}}{\partial t} \cdot 2\pi(2i + 1)\Delta r^2 \Delta z = \text{advection terms as before}$$

$$+ 2\pi(2i - 1)\frac{\Delta r^2 D \cdot 2}{\nu + wK_{\mathrm{H}}^{-1}}\left[\frac{(\nu + wK_{\mathrm{H}}^{-1})c_0^v - m(i,1)}{\Delta z}\right] \tag{127}$$

Simplification then gives

$$\frac{\partial m_{i,1}}{\partial t} = \frac{2D}{\Delta z^2}\left(c_0^v - \frac{m_{i,1}}{\nu + wK_{\mathrm{H}}^{-1}}\right) + \text{advection terms as before,}$$

$$i = 1, 1, \ldots, n_r \tag{128}$$

So in Ref. *1*, Eq. (64) is modified by the inclusion of the extra term from Eq. (128) for volume elements along the bottom of the zone of influence.

The rate at which NAPL is removed from the underlying pool is of particular interest. This is given by

$$-\frac{\partial \mathrm{NAPL}}{\partial t} = \sum_{i=1}^{n_r}\left(\frac{\partial m_{i,1}}{\partial t}\right)^{\mathrm{diff}} \cdot 2\pi(2i - 1)\Delta r^2 \tag{129}$$

and the amount of NAPL removed from the underlying pool at a time t' into a soil vapor stripping run is given by

$$(\mathrm{NAPL})_{\text{total removed}} = \int_0^{t'} \left|\frac{\partial \mathrm{NAPL}}{\partial t}\right| dt \tag{130}$$

RESULTS, NAPL REMOVAL

A computer program implementing this model was constructed by modifying a program used earlier for modeling soil vapor stripping in the presence of overlying circular caps. This program, in BASICA, was compiled and run on MMG286 microcomputer running at 10 MHz. A typical run required about an hour of computer time.

Input parameters roughly representative of wells at several sites which we had modeled previously were selected. These are given in Table 4. The

TABLE 4
Input Parameters for the Model

Height of sink above the water table	1 m
Height of ground surface above the water table	8 m
Radius of zone of influence	6 m
Well pressure, absolute	0.866 atm
Screened radius of well	0.12 m
Volumetric air flow rate at 1 atm, 20°C	0.0217 m^3/s
NAPL vapor pressure	25, 50 torr
NAPL molecular weight	86 g/mol
NAPL diffusion constant	0.005 cm^2/s
NAPL Henry's constant	0.005, 0.01
Soil temperature	20°C
Soil voids fraction	0.2
Soil Darcy's constant	0.6 $m^2/atm \cdot s$
Soil density	1.6 g/mL

plots are of $\log_{10}$ total contaminant mass in the vadose zone versus the time. The Henry's constants for the runs plotted in Fig. 15 are 0.005 and 0.01 (dimensionless); it is assumed that initially the entire vadose zone is in equilibrium with neat contaminant. Plots are of the total mass of contaminant in the vadose zone, neglecting that which is present in a bottom layer of thickness $\Delta z/2$, in which diffusion is of major importance. Note that, since the vapor pressures and molecular weights are the same in these two runs, the fluxes of NAPL from the underlying layer are the same. These are about 4.4 kg/day. As before, increasing the Henry's constant increases the rate of removal; here, however, it also increases almost proportionately the total quantity of contaminant present in the vadose zone.

Decreasing the vapor pressure of the NAPL from 50 to 25 torr while holding all other parameters constant has the effects shown in Fig. 16. Of particular importance is the fact that, as one would expect, the steady-state flux of NAPL from the bottom of the zone of influence is decreased by 50%. Obviously, the removal of NAPL of low vapor pressure by soil vapor stripping is likely to be unprofitable.

In all these runs the thickness of the diffusion boundary layer above the NAPL surface was taken to be 0.5 $m(\frac{1}{2}\Delta z)$. This is probably a rather conservatively large estimate; flux from the NAPL layer is proportional to $1/\Delta z$, so we see that these calculations should yield a lower bound for the rate of NAPL removal.

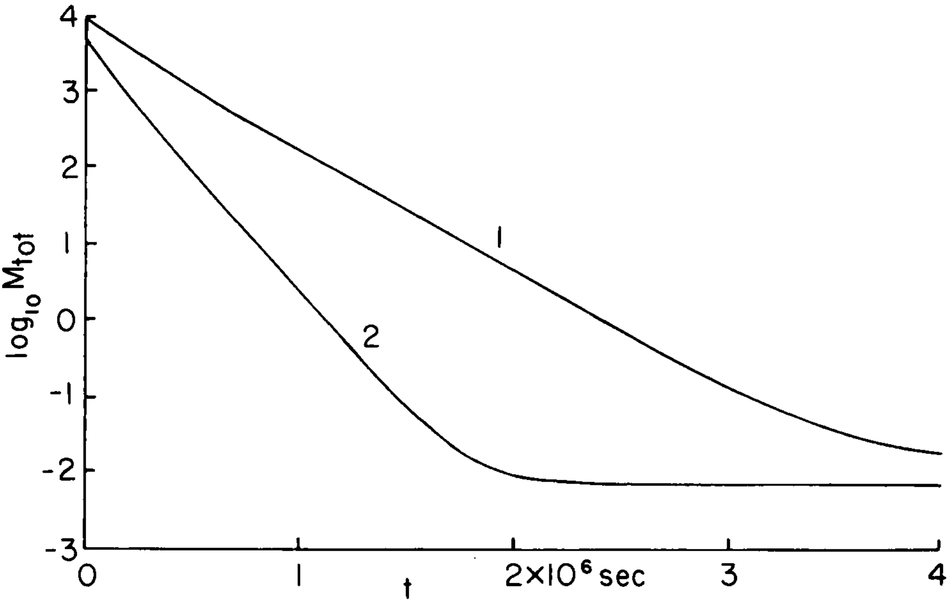

FIG. 15. Plots of $\log_{10}$ total contaminant mass (kg) in the vadose zone versus time. Henry's constant = 0.01 (upper curve), 0.005 (lower curve); other parameters as in Table 4.

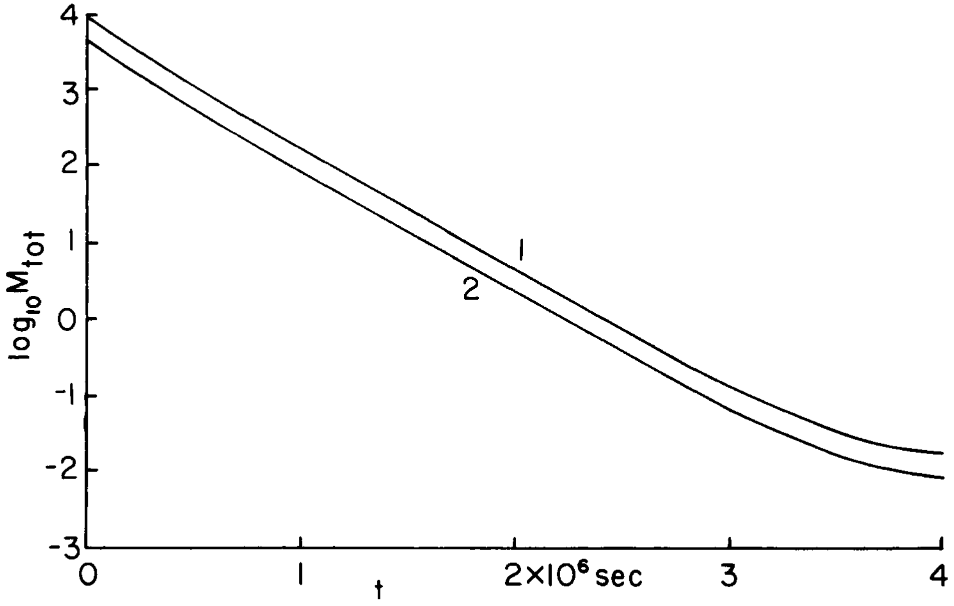

FIG. 16. Plots of $\log_{10}$ total contaminant mass (kg) in the vadose zone versus time. NAPL vapor pressure = 50 torr (upper curve), 25 torr (lower curve); other parameters as in Table 4.

In conclusion, we have shown that removal rates of NAPL underlying the vadose zone can be expected to be of the order of 2 to 5 kg/day per vapor stripping well if the wells are screened only near the bottom and extend down to within half a meter or so of the NAPL layer. This should be helpful to the environmental engineer confronted with the task of removing NAPL beneath the vadose zone. This technique can be expected to be useless for removing DNAPL lying beneath the surface of the zone of saturation, since diffusion transport of the DNAPL through a water layer of any appreciable thickness will be extremely slow.

Acknowledgment

D.J.W. is indebted to the Water Resources Research Center of the University of Tennessee for a grant in partial support of this work.

REFERENCES

1. D. J. Wilson, A. N. Clarke, and J. H. Clarke, *Sep. Sci. Technol., 23,* 991 (1988).
2. K. Gannon, D. J. Wilson, A. N. Clarke, R. D. Mutch Jr., and J. H. Clarke, *Ibid., 24,* 831 (1989).
3. W. L. Wootan Jr. and T. Voynick, *Forced Venting to Remove Gasoline Vapor from a Large-Scale Aquifer,* Submitted by Texas Research Institute to American Petroleum Institute, Washington, D.C., January 13, 1984.
4. A. N. Clarke, *Zone I Soil Decontamination through in Situ Vapor Stripping Processes,* Contract no. 68-02-4446, Final Report to EPA, AWARE, Inc., April 1987.
5. Woodard Clyde Consultants, *Performance Evaluation Pilot Scale Installation and Operation, Soil Installation and Operation, Soil Gas Vapor Extraction System, Time Oil Company Site, Tacoma, Washington, South Tacoma Channel, Well 12A Project,* Work Assignment no. 74-0N14.1, Walnut Creek, California, December 13, 1985.
6. G. J. Anastos, P. J. Parks, M. H. Corbin, and M. F. Coia, *In Situ Air Stripping of Soils Pilot Study,* Submitted by Roy F. Weston, Inc., to U.S. Army Toxic and Hazardous Materials Agency, Aberdeen Proving Ground, Maryland, Report AMXTH-TE-TR-85026, October 1985.
7. W. L. Crow, E. P. Anderson, and E. Minugh, *Subsurface Venting of Hydrocarbon Vapors from an Underground Aquifer,* Submitted by Riedel Environmental Services Co. and Radian Corp. to American Petroleum Institute, Washington, D.C. API Publication No. 4410, 1985.
8. R. E. Bailey and D. Gervin, "In Situ Vapor Stripping of Contaminated Soils: A Pilot Study," in *Proc., 1st Annu. Hazardous Materials Management Conf./Central,* 1988, p. 207.
9. H. J. Lord, "Activated Carbon Treatment of Contaminants from a Soil Venting Operation: A Case Study," in *Proc., 1st Annu. Hazardous Materials Management Conf./Central,* title only, Liberty Environmental Systems, Inc., 1988.

10. P. A. Michaels, *Technology Evaluation Report: Site Program Demonstration Test, Terra Vac In-Situ Vacuum Extraction System, Groveland, Massachusetts,* Enviresponse, Inc., Livingston, New Jersey, EPA Contract No. 68-03-3255, 1989.

11. A. N. Clarke and D. J. Wilson, "A Phased Approach to the Development of In Situ Vapor Stripping Treatment," in *Proc., 1st Annu. Hazardous Materials Management Conf./Central,* 1988, p. 191.

12. D. J. Wilson, "Mathematical Modeling of In Situ Vapor Stripping of Contaminated Soils," *Ibid.,* p. 94.

13. F. S. Shaw, *An Introduction to Relaxation Methods,* Dover, New York, 1953.

14. Texas Research Institute, Inc., *Examination of Venting for Removal of Gasoline Vapors from Contaminated Soil,* American Petroleum Institute, API Publication no. 4429, 1980.

Received by editor November 21, 1988